Structural basis for receptor sharing and activation by interleukin-20 receptor-2 (IL-20R2) binding cytokines

Naomi J. Logsdon[a], Ashlesha Deshpande[a,b], Bethany D. Harris[a], Kanagalaghatta R. Rajashankar[c], and Mark R. Walter[a,b,1]

[a]Center for Biophysical Sciences and Engineering and [b]Department of Microbiology, University of Alabama, Birmingham, AL 35294; and [c]Northeastern Collaborative Access Team, Department of Chemistry and Chemical Biology, Cornell University, Argonne, IL 60439

Edited by Pamela J. Bjorkman, California Institute of Technology, Pasadena, CA, and approved June 7, 2012 (received for review October 24, 2011)

Interleukin 20 (IL-20) is a pleotropic IL-10 family cytokine that protects epithelial surfaces from pathogens. However, dysregulated IL-20 signaling is implicated in several human pathologies including psoriasis, rheumatoid arthritis, atherosclerosis, and osteoporosis. IL-20, and related cytokines IL-19 and IL-24, designated IL-20 subfamily cytokines (IL-20SFCs), induce cellular responses through an IL-20R1/IL-20R2 (type I) receptor heterodimer, whereas IL-20 and IL-24 also signal through the IL-22R1/IL-20R2 (type II) receptor complex. The crystal structure of the IL-20/IL-20R1/IL-20R2 complex reveals how type I and II complexes discriminate cognate from noncognate ligands. The structure also defines how the receptor–cytokine interfaces are affinity tuned to allow distinct signaling through a receptor complex shared by three different ligands. Our results provide unique insights into the complexity of IL-20SFC signaling that may be critical in the design of mechanistic-based inhibitors of IL-20SFC–mediated inflammatory disease.

Interleukin 20 (IL-20) is an α-helical cytokine discovered by EST database mining and mapped to human chromosome 1q32 in a cluster with IL-10, IL-19, and IL-24 (MDA7) (1). On the basis of genomic location, amino acid sequence identity (32–40%), and use of a common receptor chain for signaling (IL-20R2), IL-19, IL-20, and IL-24 have been designated as IL-20 subfamily cytokines (SFCs) (2, 3). The IL-20 SFCs, IL-10, IL-22, and IL-26 form the IL-10 cytokine family, which together with the interferons (type I, IFN-α/β; type II, IFN-γ; and type III, IFN-λs or IL-28/IL-29) form the class 2 cytokine family (1, 4, 5).

IL-20 SFCs induce cellular signaling through a common receptor heterodimer composed of IL-20R1 and IL-20R2 chains (type I complex) (Fig. 1) (1, 6, 7). IL-20 and IL-24 also signal through an IL-22R1/IL-20R2 heterodimer (type II complex), whereas IL-19 only signals through the type I complex (6, 7). IL-20R1 and IL-22R1 also pair with the IL-10R2 chain to form receptor heterodimers that induce cell signaling upon IL-26 (IL-20R1/IL-10R2) and IL-22 (IL-22R1/IL-10R2) binding, respectively (8–10). Despite promiscuous pairing of the R2 chains, IL-20R2 cannot substitute for IL-10R2 in IL-22 signaling (6). Furthermore, IL-19, IL-20, and IL-24 appear to have largely nonredundant biological activities in vivo, suggesting they may engage type I and type II receptor heterodimers differently (6, 7, 11). However, a mechanistic basis for such differences has not been determined.

IL-20 has been implicated in the pathophysiology of psoriasis (1). Transgenic (Tg) mice overexpressing IL-20 exhibit a phenotype similar to human psoriatic skin, and IL-20 neutralizing antibodies resolve psoriasis in a human xenograft transplation model (1, 12). Increased levels of IL-19 and IL-24 are also observed in skin samples from psoriasis patients, but the significance and/or biological function of IL-19 and IL-24 is less clear (3). IL-24 Tg mice exhibit epidermal hyperplasia and proliferation, suggesting IL-24 activity in vivo is similar to IL-20 (13). However, IL-19 Tg mice were reported to exhibit a normal skin phenotype, which is consistent with IL-19's unique receptor specificity. IL-20 is also implicated in rheumatoid arthritis (RA) (14) and atherosclerosis (15). IL-20 also exhibits arteriogenic/angiogenic properties and may be important for treating ischemic disease (16). Most recently, IL-20 was found to induce osteoclastogenesis, by up-regulating the receptor activator of NFκB (RANK)–RANK ligand signaling proteins and may be a therapeutic target for osteoporosis (17).

Expression of the IL-20R1/IL-20R2 and IL-22R1/IL-20R2 heterodimers, which are required for IL-20 bioactivity, have been observed only on cells of epithelial origin including skin, lung, and testis (1, 18, 19). These data suggest a major role for IL-20 SFCs in mediating cross-talk between infiltrating immune cells (T cells, macrophages, and dendritic cells) that express the IL20SFCs, and the skin. However, in some cases the pleotropic activities of IL-20 are at odds with the cellular expression of the IL-20 receptors. In particular, IL-20 and IL-19 induce naïve T cells toward a TH2 secretory phenotype, characterized by increased IL-4, IL-13, and reduced IFNγ production (20, 21). However, only IL-20R2 but not IL-20R1 or IL-22R1 have been detected in immune cells (1, 18, 19). In addition, IL-20R2 knockout mice exhibit disrupted $CD4^+$ and $CD8^+$ T-cell function (22), which implicates the IL-20 SFCs in T-cell signaling, despite the absence of the IL-20R1 and IL-22R1 receptor chains on these cells (18). On the basis of these data, it has been hypothesized that another receptor chain must pair with IL-20R2 to induce IL-20SFC signaling on immune cells.

IL-20 has emerged as a highly pleotropic cytokine involved in essential cellular processes and pathology. Despite an improved understanding of IL-20 biology, the molecular mechanisms that allow IL-20, IL-19, and IL-24 to discriminate and activate type I (IL-20R1/IL-20R2) and type II (IL-22R1/IL-20R2) receptor complexes are currently unknown. To address this question, we have determined the crystal structure of the IL-20/IL-20R1/IL-20R2 complex to determine how signaling complexity can be obtained for structurally similar cytokines.

Results

Overall Architecture of the IL-20/IL-20R1/IL-20R2 Signaling Complex. The structure of IL-20/IL-20R1/IL-20R2 (Fig. 2*A*) was solved at 2.8 Å by single wavelength anomalous diffraction phasing and molecular replacement methods (Table S1). IL-20 adopts an α-helical fold, which is highly conserved with IL-19 (rmsd 0.79 Å). Despite structurally similar helical cores, the N terminus of IL-20 adopts a novel β-hairpin structure, rather than the 3^{10} helix/coil structure observed in IL-19 (Fig. 2*B*). Threading the IL-24 amino acid sequence onto the structure of IL-20 suggests IL-20 and IL-24 adopt similar N-terminal β-hairpin structures, which positions $Cys\text{-}59^{IL\text{-}24}$ and $Cys\text{-}106^{IL\text{-}24}$ in close proximity (Cα–Cα distance = 6.6 Å) for disulfide bond formation (*SI Materials and*

Author contributions: N.J.L., A.D., B.D.H., K.R.R., and M.R.W. designed research; N.J.L., A.D., B.D.H., K.R.R., and M.R.W. performed research; N.J.L., A.D., K.R.R., and M.R.W. analyzed data; and M.R.W. wrote the paper.

The authors declare no conflict of interest.

This article is a PNAS Direct Submission.

[1]To whom correspondence should be addressed. E-mail: walter@uab.edu.

This article contains supporting information online at www.pnas.org/lookup/suppl/doi:10.1073/pnas.1117551109/-/DCSupplemental.

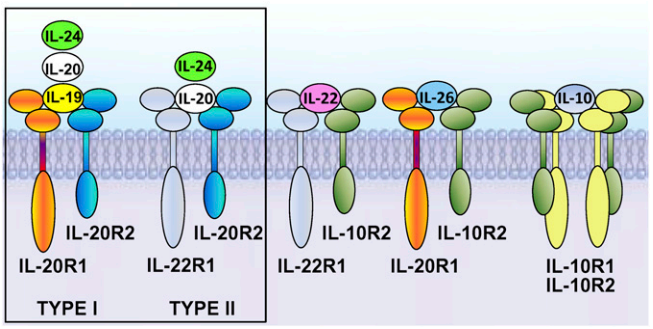

Fig. 1. Schematic diagram of IL-10 family receptor complexes. The box distinguishes IL-20R2 signaling complexes from IL-10R2 complexes, which use identical R1 chains.

Methods, Fig. S1). Thus, the predicted structural similarity of IL-20 and IL-24 is consistent with the identical receptor binding profiles of each cytokine (Fig. 1).

The extracellular fragments of IL-20R1 and IL-20R2 each consist of tandem β-sandwich domains (D1 and D2) that assemble around IL-20 to form a V-shaped complex, when viewed down the α-helical bundle axis of IL-20 (Fig. 2*A*). X-ray analysis of IL-20R1 and IL-20R2 completes the structural descriptions of all five IL-10 family receptors (23–26) (Fig. 1). Structural comparisons of the receptors reveal the three R1 chains are highly similar to one another, whereas IL-10R2 and IL-20R2 exhibit structurally divergent cytokine binding loops and interdomain angles (Fig. 2*C* and *SI Materials and Methods* and Fig. S2).

IL-20/IL-20R1/IL-20R2 ternary complex formation is mediated by three protein interfaces, IL-20/IL-20R1 (site 1), IL-20/IL-20R2 (site 2), and IL-20R1/IL-20R2 (site 3), that bury a total of 4,236 Å^2 of accessible surface area (Fig. 2*A*). The IL-20/IL-20R1 site 1 interface (1,576 Å^2) consists of two contact surfaces, site 1a and site 1b (Fig. 3*A*). Site 1a is formed by IL-20R1 L2–L4 loops that contact a small cavity on IL-20 located at the intersection of helix F and AB loop. Site 1b contacts occur between IL-20R1 L6 and the N terminus of helix A. Site 1a contributes ~83% of the total buried surface area and eight of nine hydrogen bond (H-bond)/salt bridge interactions identified in the IL-20/IL-20R1 interface (Table S2 and Fig. 3). In contrast to site 1a, site 1b is very small and made up almost entirely of IL-20R1 L6 residues Gly-224$^{IL\text{-}20R1}$, Pro-225$^{IL\text{-}20R1}$, and Pro-226$^{IL\text{-}20R1}$, which form Van der Waal contacts with the aliphatic portion of Arg-43$^{IL\text{-}20}$ and a single hydrogen with helix A residue Gln-40$^{IL\text{-}20}$.

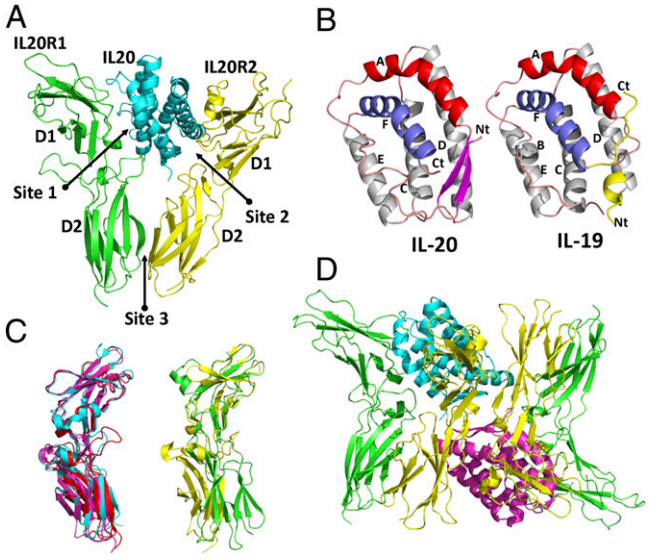

Fig. 2. IL-20/IL-20R1/IL-20R2 ternary complex. (*A*) Ribbon diagram of the IL-20 ternary signaling complex. (*B*) Ribbon diagram of IL-19 and IL-20, with unique N-/C-terminal regions colored yellow and magenta, respectively. (*C*) Superposition of the R1 chains, IL-10R1 (cyan), IL-20R1 (red), and IL-22R1 (magenta), on the *Left* and R2 chains, IL-10R2 (yellow) and IL-20R2 (green) on the *Right*. (*D*) The IL-20 dimeric complex observed in the asymmetric unit of the crystals (*SI Materials and Methods* and Fig. S3).

The site 2 IL-20/IL-20R2 interface (1,624 Å^2) is centered on IL-20 helix D, which is surrounded by IL-20R2 L2 and L3 loops (Fig. 4). The IL-20R2 L2 loop also makes significant contacts with helix C, via Tyr-74$^{IL\text{-}20R2}$, whereas residues on L4 and L5 loops form hydrogen bonds with helix A and the IL-20 N terminus. As observed in site 1a, the IL-20R2 L2 loop forms the majority of contacts in site 2 by contributing 57% of the buried surface area, and 9 of 13 hydrogen bonds in the IL-20/IL-20R2 interface (Table S3). Six of these hydrogen bonds are formed with helix D residues Ser-110$^{IL\text{-}20}$, Ser-111$^{IL\text{-}20}$, and Asn-114$^{IL\text{-}20}$, which are conserved in the sequences of IL-19 and IL-24 (Fig. 4*B* and *SI Materials and Methods* and Fig. S1). Thus, IL-20R2, and the IL-20SFCs share a conserved binding epitope to facilitate promiscuous IL-20R2 ligand engagement (Fig. 1).

Essentially all contacts between IL-20 and the receptors are mediated by the D1 domains, whereas IL-20R1 and IL-20R2 D2 domains contact one another to form the base of the V-shaped complex (site 3, Figs. 2*A* and 5*A*). The site 3 interface (1,036 Å^2) is formed from IL-20R1 D2 residues on β-strand C′, the CC′ loop, and the EF loop, which contact IL-20R2 residues on the AB loop, β-strand E, and the EF loop. The interface is quite extensive, including 6 hydrogen bonds (Table S4) contributed predominantly from the AB loop of IL-20R2 and the EF loop of IL-20R1.

IL20/IL-20R1/IL-20R2 Dimer Complex. Two 1:1:1 IL-20/IL-20R1/IL-20R2 complexes form a dimer in the asymmetric unit of the crystals (Fig. 2*D*). The IL-20 dimer interface is very small (~200 Å^2), consistent with IL-20 being a monomer in solution. The dimer is stabilized by contacts formed between IL-20R2 chains that bridge the twofold related IL-20s. Each IL-20R2 forms a site 2 interface (Figs. 2*A* and 4 and Table S5), and a second contact between IL-20R2 D2 domain and IL-20 helix D (residues 121–130, Fig. S3). The IL-20/IL-20R2 dimer interface is extensive, burying 1,982 Å^2 of accessible surface area. Two IL-20R1 chains are also in the complex, but they do not contribute residues to the dimer interface. Although the formation of cell surface IL-20R2 dimers might provide an explanation for IL-20SFC signaling on immune cells that apparently lack IL-20R1 (27), we have been unable to detect an IL-19/IL-20R2 dimeric complex in solution or identify significant differences in IL-20SFC binding affinity between monomeric and dimeric IL-20R2 (*SI Materials and Methods*, Fig. S4 and Table S6).

Mechanisms Regulating IL-20R1 Chain Affinity. Surface plasmon resonance (SPR) experiments were performed to quantify IL-20R1 binding to IL-19 and IL-20 (Fig. 6). We could not detect binding between IL-19 and IL-20R1 at IL-19 concentrations up to 10 μM. However, a binding constant of ~9 μM was determined for the IL-20/IL-20R1 interaction (Fig. 6*B*). In contrast to very weak IL-20R1 interactions, IL-10R1 and IL-22R1 chains exhibit ~10,000-fold tighter binding affinity for IL-10 (kDa = 0.5 nM) and IL-22 (kDa = 1.2 nM) (24, 28) (Fig. 1). These extremely different binding affinities occur despite structurally similar IL-20/IL-20R1, IL-22/IL-22R1, and IL-10/IL-10R1 binary complexes (Fig. 3*B*). Comparison of each interface reveals identical "YG" interaction motifs consisting of receptor YG residues (L2 loop Tyr-76$^{sIL\text{-}20R1}$ and Gly-77$^{sIL\text{-}20R1}$ in IL-20R1, Fig. 3*A*) that are inserted into a conserved cleft formed by the AB loop and

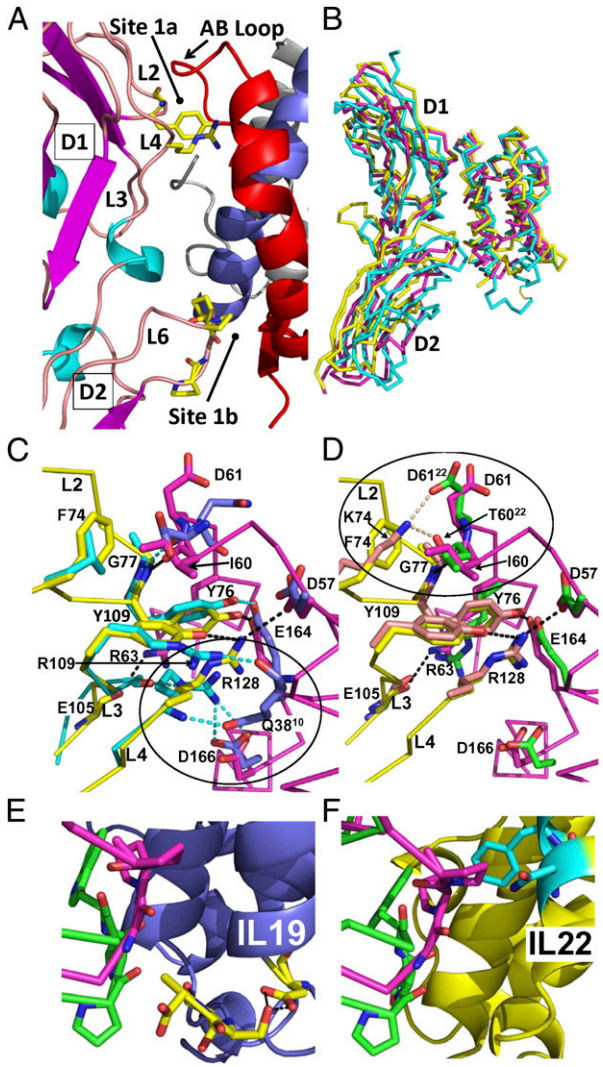

Fig. 3. Site 1 interface: structure, affinity, and specificity. (*A*) Ribbon diagram of the IL-20/IL-20R1 interface. (*B*) Superposition of IL-10/IL-10R1 (cyan), IL-20/IL-20R1 (yellow), and IL-22/IL-22R1 (magenta) binary complexes. (*C*) Comparison of site 1a between IL-10/IL-10R1 (cyan) and IL-20/IL-20R1 (yellow). IL-20 and selected residues are colored magenta. Residues corresponding to IL-10 are colored purple and shown on the IL-20 scaffold. Dashed lines in the circle, colored cyan, are IL-10–specific hydrogen bonds. Black dashed lines correspond to IL-20/IL-20R1 hydrogen bonds. (*D*) Comparison of site 1a between IL-22/IL-22R1 (tan) and IL-20/IL-20R1 (yellow). IL-20 is colored as in *C*. IL-22 residues are green and shown on the IL-20 scaffold. Dashed lines in the circle, colored tan, are IL-22–specific hydrogen bonds. Black dashed lines correspond to hydrogen bonds conserved in IL-20 and IL-22 interfaces. (*E* and *F*) Site 1b steric clashes observed for noncognate complexes (Fig. 1). IL-19 (*E*) clashes with IL-22R1 L6 loop (green), but not IL-20R1 L6 (magenta). IL-22 (*F*) clashes with the IL-20R1 L6 loop (magenta), but not IL-22R1 L6 (green).

helix F of the ligands (Fig. 3 *C* and *D*) (23, 24, 26). Buried surface area does not predict the observed affinities of the different complexes (Table S7). However, complex affinities correlate with unique contacts made by four receptor residues (D1 residues Phe-74 (L2 loop), Glu-105 (L3 loop), Tyr-109, and Arg-128 (L4 loop) in IL-20R1, Fig. 3 *C* and *D*; for clarity, IL-20R1 numbering will be used throughout the text), located adjacent to the YG interaction motif (Fig. 3 *C* and *D*).

In the high-affinity IL-10/IL-10R1 complex, Arg-109$^{IL\text{-}10R1}$ and Arg-128$^{IL\text{-}10R1}$, adjacent to the YG motif, form a network of four hydrogen bonds with IL-10 residues Gln-38$^{IL\text{-}10}$ and Asp-166$^{IL\text{-}10}$ (Fig. 3*C*). However, in IL-20/20R1 and IL-22/IL-22R1 interfaces, Arg109$^{IL\text{-}10R1}$ is replaced with Tyr-109$^{IL\text{-}20R1,\ IL\text{-}22R1}$, which no longer contacts IL-20 or IL-22 directly, but repositions Arg-128$^{IL\text{-}20R1,\ IL\text{-}22R1}$ for interactions with Asp-57$^{IL\text{-}20,\ IL\text{-}22}$, despite the fact Asp-166 is conserved in IL-20 and IL-22 (Fig. 3*D*). Thus, this network of four hydrogen bonds in the IL-10/IL-10R1 interface is reduced to one in IL-20/IL-20R1 and IL-22/IL-22R1 interfaces.

To compensate for the loss of an "IL-10 like" bonding network, the IL-22/IL-22R1 interface forms a unique three hydrogen bond network on the opposite side of the YG motif (Fig. 3*D*). This interaction includes hydrogen bonds between Arg-63$^{IL\text{-}22}$ and Glu-105$^{IL\text{-}22R1}$ and between IL-22R1 L2 loop residue, Lys-74$^{IL\text{-}22R1}$, and IL-22 AB loop residues Thr-60$^{IL\text{-}22}$ and Asp-61$^{IL\text{-}22}$. Mutation of Lys-74$^{IL\text{-}22R1}$ to alanine reduces IL22 functional activity by ~100-fold, supporting a critical role for this bonding network in IL-22/IL-22R1 interactions (26).

Consistent with its low affinity and in contrast to IL-10/IL-10R1 and IL-22/IL-22R1, the IL-20/IL-20R1 complex does not form additional site 1a hydrogen bonding networks (Fig. 3*D*). Lys-74$^{IL\text{-}22R1}$, the key residue in the IL-22/IL-22R1 interface, is replaced by Phe-74$^{IL\text{-}20R1}$ and Thr-60$^{IL\text{-}22}$ is replaced with Ile-60$^{IL\text{-}20}$. Thus, the IL-20/IL-20R1 site 1a interface consists of the YG motif and two additional hydrogen bonds (Arg-128$^{IL\text{-}20R1}$/Asp-57$^{IL\text{-}20}$ and Glu-105$^{IL\text{-}20R1}$/Arg-63$^{IL\text{-}20}$) that are conserved with IL-22/IL-22R1. Additional disruption of these interactions is predicted in the lower affinity IL-19/IL-20R1 interface where IL-20 residues Ile-60$^{IL\text{-}20}$ and Arg63$^{IL\text{-}20}$ are replaced by Pro-60$^{IL\text{-}19}$ and Thr63$^{IL\text{-}19}$ in IL-19.

Mechanisms Regulating IL-20R2 Binding to IL-19 and IL-20. Additional SPR experiments reveal IL-19 binds tighter to IL-20R2 (kDa =

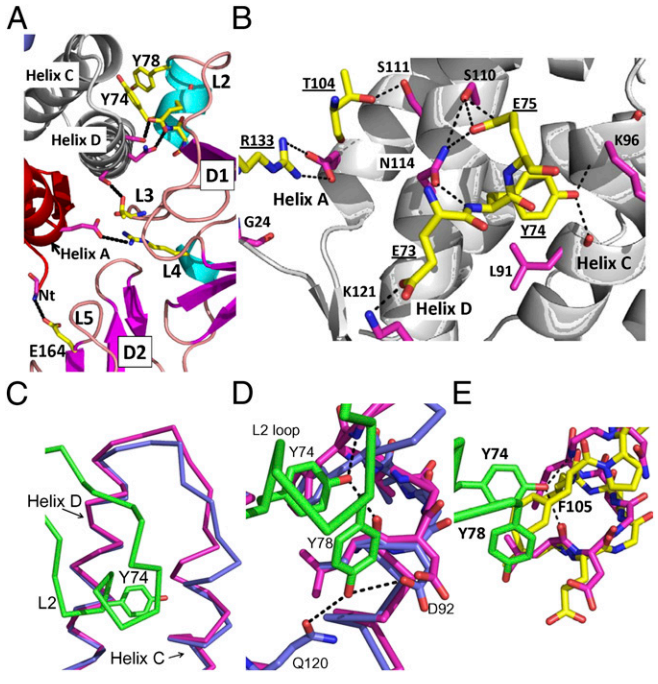

Fig. 4. IL-20 site 2 interface: mechanisms controlling affinity and specificity. (*A*) Ribbon diagram of the IL-20/IL-20R2 interface. (*B*) Detailed contacts in the IL-20/IL-20R2 site 2 interface. (*C*) Conformational differences in helix C between IL-20 bound to IL-20R2 (magenta) and unbound IL-19 (blue). The IL-20R2 L2 loop (green) is also shown. (*D*) Contacts between IL-19 (blue) and IL-20R2 (green), not found in IL-20 (magenta)/IL-20R2, that modulate increased IL-19/IL-20R2 affinity. (*E*) Specificity mechanism preventing noncognate IL-22 (yellow) from binding to IL-20R2 (green) is controlled by IL-22 helix D residue, Phe-105$^{IL\text{-}22}$. Cognate IL-20 (magenta) is also shown (Fig. 1).

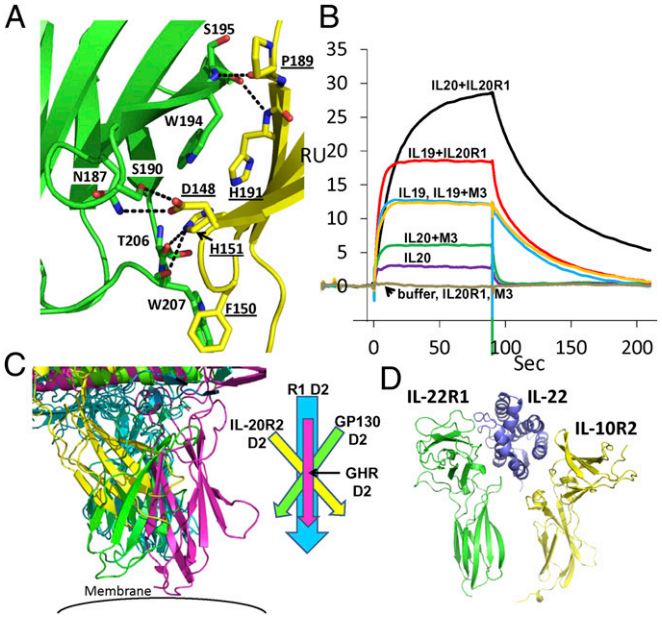

Fig. 5. IL-20 site 3 interface is essential and distinct from other complexes. (*A*) Site 3 interface with IL-20R1 colored green and IL-20R2 colored yellow. (*B*) Importance of the site 3 interface in ternary complex formation. SPR sensograms obtained by injecting cytokines (IL-19 or IL-20, at 250 nM) and/or receptors (IL-20R1 or M3, at 425 nM), as labeled, over an IL-20R2 coupled biacore chip. Injection of IL-20+IL-20R1 (black line) results in a large response, consistent with ternary complex formation. However, injection of IL-20+M3 (green line), an IL-20R1 site 3 mutant with S190$^{IL\text{-}20R1}$, W194$^{IL\text{-}20R1}$, and W207$^{IL\text{-}20R1}$ (*A*) mutated to alanine, drastically reduces binding due to disruption of ternary complex formation. Similar results are observed for complex formation by IL-19. (*C*) Superposition of the D2 domains of GHR site 1, IL-6R, and IL-20R1 (cyan). The positions of the D2 domains of GHR site 2 (magenta), GP130 (green), and IL-20R2 (yellow) are shown, along with a schematic of the differences in their orientations. (*D*) Putative model of the IL-22/IL-22R1/IL-10R2 complex based on the IL-20 ternary complex structure (Fig. 2*A*, *SI Materials and Methods* and Fig. S5). The D2 domains of the model are separated by 15Å, suggesting IL-10R2 complexes are distinct from IL-20R2 complexes.

105 nM) than IL-20 (kDa = 697 nM) (Fig. 6 *C* and *D*). Superposition of unbound IL-19 onto IL-20 in the ternary complex, reveals most interactions observed in the IL-20/IL-20R2 interface (Fig. 4*B* and Table S2) are conserved in the IL-19/IL-20R2 complex. However, helix C adopts a different conformation (~3 Å changes) in IL-19, relative to IL-20 bound to IL-20R2 (Fig. 4*C*). The conformation of helix C in IL-19 positions Asp-92$^{IL\text{-}19}$ into hydrogen bonding distance (3.5 Å) with the OH of Tyr-78$^{IL\text{-}20R2}$, whereas the equivalent residue in IL-20 (Asp-92$^{IL\text{-}20}$) is 4.3 Å from Tyr-78$^{IL\text{-}20R2}$ (Fig. 4*D*). Replacement of IL-20 Lys-120$^{IL\text{-}20}$ with Gln-120$^{IL\text{-}19}$ in IL-19 forms an additional hydrogen bond Tyr-78$^{IL\text{-}20R2}$ in the IL-19/IL-20R2. The additional hydrogen bonds in the IL-19/IL-20R2 interface are consistent with the higher affinity of this complex than IL-20/IL-20R2 (Fig. 6 *C* and *D*). The structural differences between IL-19 and IL-20 demonstrate helix C and the CD loop are conformationally dynamic, which may also influence IL-20R2 binding affinity.

Structural Mechanisms Regulating Cognate vs. Noncognate Ligand Specificity. IL-20R1 and IL-22R1 form promiscuous interactions with five different cytokines and two R2 chains to engage different signaling responses that protect the host from invading pathogens (Fig. 1). These cognate ligand receptor complexes have been "affinity tuned," using mechanisms described above, to optimize their signaling properties. However, IL-19 cannot bind or signal through the IL-22R1 chain. Furthermore, IL-22 cannot bind or induce signaling through the IL-20R1 chain (Fig. 1). Superposition of IL-22 onto IL-20/IL-20R1 reveals the major specificity determinant is site 1b, where the IL-20R1 L6 loop forms steric clashes with IL-22 helix A residues Phe-57$^{IL\text{-}22}$ and Asn-54$^{IL\text{-}22}$ (Fig. 3*F*). Similar clashes are observed between IL-22R1 L6 and the N terminus of IL-19 (Fig. 3*E*), which explains why IL-19 cannot signal through the type II complex (Fig. 1). Thus, although cognate site 1b contacts are not always extensive, they are clearly critical in determining ligand–receptor specificity. These results provide additional evidence for a two-point (site 1a/site 1b) R1 chain specificity mechanism described by Jones et al. (24).

Signaling specificity is also achieved through the IL-20R2 chain, which must engage IL-19, IL-20, and IL-24, but prevent IL-22 signaling through the type II (IL-22R1/IL-20R2) complex (Fig. 1) Because IL-22 can signal through the IL-22R1/IL-10R2 heterodimer, but not the IL-22R1/IL-20R2 complex (6), specificity must occur in the IL-22/IL-20R2 interface. To test this hypothesis, IL-22 was positioned onto IL-20 in the IL-20 ternary complex. This experiment positions IL-22 helix C residue, Phe-105$^{IL\text{-}22}$, at the center of the site 2 interface, where it forms extensive steric clashes with IL-20R2 residues Tyr-74$^{IL\text{-}20R2}$ and Tyr-78$^{IL\text{-}20R2}$ (Fig. 4*E*). These steric disruptions would prevent noncognate IL-22/IL-20R2 interactions and subsequent cellular signaling by this complex.

Importance of the Site 3 Interface in Complex Formation and Signaling. The low affinity of IL-20R1 and IL-20R2 binary complexes emphasizes the importance of the site 3 interface (Figs. 2A and 5A) in forming signaling competent ternary complexes. To estimate the stability of IL-20 (IL-20/IL-20R1/IL-20R2 and IL-20/IL-22R1/IL-20R2) and IL-19 (IL-19/IL-20R1/IL-20R2) ternary complexes (Fig. 1), IL-19 or IL-20 was coinjected with soluble IL-20R1 over a biacore chip coupled with IL-20R2. The apparent affinities obtained from the coinjection experiments (Fig. 6 *E–H*) suggest the IL-20 type I complex (Fig. 1) is the most stable complex with apparent equilibrium dissociation constant (KDapp) of 319 nM, followed by the IL-20 type II complex (KDapp = 1,363 nM), and then the IL-19/IL-20R1/IL-20R2 complex (KDapp = 3,121 nM). The same results, although with different KDapp values, were obtained by evaluating ternary complex stability by injecting soluble IL-20R2 and IL19, or IL-20, over biacore chip surfaces of IL-20R1 or IL-22R1 (*SI Materials and Methods* and Fig. S5).

To further test the importance of the site 3 interface, three IL-20R1 site 3 residues that form site 3 contacts (Fig. 5*A*, Ser-190^{IL20R1}, Trp- 194$^{IL\text{-}20R1}$, and Trp-207$^{IL\text{-}20R1}$) were mutated to alanine to create an IL-20R1 triple mutant, M3. Coinjection of IL-19+M3 over an IL-20R2 biacore surface, generated the same binding response as IL-19 alone (Fig. 5*B*). Coinjection of IL-20+M3 exhibited an increased binding response, relative to IL-20 alone, although it was drastically reduced from the injection of IL-20+IL-20R1. The increased binding observed for the IL-20+M3 injection corresponds to IL-20/M3 binary complexes binding to IL-20R2 with the same kinetics as the IL-20/IL-20R2 interaction (e.g., without the site 3 interaction). This result confirms the higher affinity of the IL-20/IL-20R1 site 1 interface (Fig. 6 *A* and *B*), relative to IL-19/IL-20R1, and the importance of site 3 in forming stable ternary complexes essential for signal transduction.

The essential role of the site 3 interface in IL-20 ternary complex formation, led us to examine how the IL-20R1/IL-20R2 D2/D2 interface (site 3) differed from other cytokine ternary complexes. To ask this question, the D2 domains of growth hormone receptor (GHR, site 1) (29) and IL-6R (30) were superimposed onto IL-20R1 D2 and the orientations of GHR (site 2) and GP130 D2 domains were evaluated (Fig. 5*C*). The GHR/GHR D2 domains are essentially parallel to one another and were assigned a D2–D2 crossing angle of 0°. Compared with

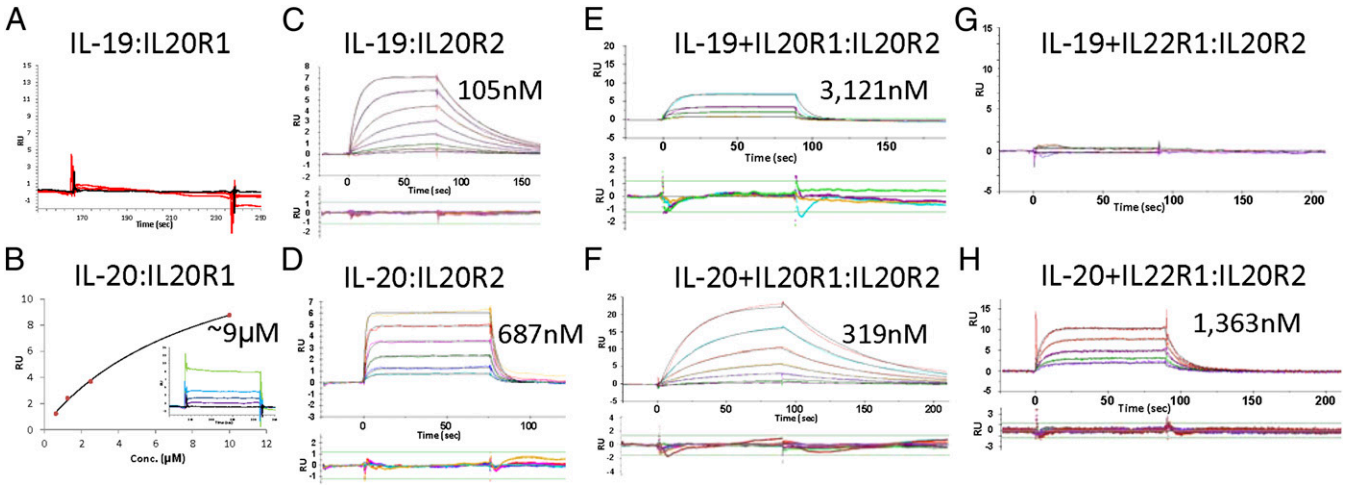

Fig. 6. IL19/IL-20 receptor interactions and complex stability. SPR sensorgrams, data fit (black lines), equilibrium dissociation constant values, and residual errors obtained for complexes described at the *Top* of each panel. Panels are labeled as injected soluble proteins, followed by a semicolon (:), then the protein coupled to chip surface, IL-20R1 or IL-20R2. (*A* and *B*) Injection of IL-19 and IL-20 (maximum concentration, max conc. = 10 μM, twofold diluted to 0.625 μM) over IL-20R1. (*C* and *D*) Injection of IL-19 (max conc. = 500 nM, twofold diluted to 3.91 nM) or IL-20 (max conc. = 2,000 nM, twofold diluted to 62.5 nM) over IL-20R2. (*E*–*H*) IL-19 and IL-20 (fixed at 250 nM) were mixed with different concentrations of IL-20R1 or IL-22R1, (max conc. = 1,000 nM, twofold diluted to 7.81 nM) and injected over IL-20R2. To estimate R1 chain affinity/complex stability, the contribution of the ligand was removed by using the 250 nM IL-19 or IL-20 sensorgram as the blank subtraction. All sensorgrams were fit to 1:1 binding models. Kinetic parameters are listed in Table S6.

GHRs, the D2 domains of IL-20R1/IL-20R2 and IL-6R/GP130 D2 cross at angles of −40° and +25°, respectively (Fig. 5*C*). These differences may be important as the D2 domains are located adjacent to the membrane where they could selectively influence intracellular signal transduction pathways and ultimately cellular responses.

Not only is the IL-20/IL-20R1/IL-20R2 complex distinct from the distantly related class-1 cytokine complexes, but it is also distinct from IL-10R2-containing complexes (Fig. 1). For example, superposition of the IL-22/IL-22R1 binary complex and IL-10R2 onto IL-20/IL-20R1/IL-20R2 results in a IL-22/IL-22R1/IL-10R2 complex that does not form a site 3 interface (Fig. 5*D*). This result is caused by the distinct interdomain angle of IL-20R2 compared with IL-10R2 (*SI Materials and Methods* and Fig. S2). To determine whether IL-10R2 adopts a different interdomain angle in solution, compared with the crystal structure (25), solution small angle X-ray scattering (SAXS) was performed on IL-10R2. These experiments confirm that IL-10R2 in solution adopts the same D1/D2 interdomain angle observed in the crystal structure (Fig. S6). These studies further underscore the unique architectures of the IL-20R2 and IL-10R2 ternary complexes and their distinct assembly properties.

Discussion

The crystal structure of IL-20/IL-20R1/IL-20R2 depicts a complete signaling complex of an IL-10 family cytokine, although two binary complexes (IL-10/IL-10R1 and IL-22/IL-22R1) have been determined (23, 24, 26). The surprising structural differences between IL-19 and IL-20 at the N- and C termini (*SI Materials and Methods* and Fig. S1) explains how structurally similar cytokines discriminate, via IL-20R1 and IL-22R1, between the type I and type II receptor heterodimers (Fig. 4 *E* and *F*). In contrast, IL-22, which binds tightly to IL-22R1 (24), cannot signal through the type II complex due to steric clashes between IL-22/IL-20R2 in site 2, especially with Phe-105$^{IL\text{-}22}$ (Fig. 5*E*). These results provide a structural basis for IL-20SFC receptor specificity, which contributes to their distinct in vivo biological properties.

In addition to discriminating between the type I and type II complexes (Fig. 1), IL-19 and IL-20 modulate their biological activities through distinct affinities for IL-20R1 and IL-20R2 chains (Fig. 6). Our structural studies now provide a molecular basis for how subtle structural rearrangements of the receptor interfaces, combined with amino acid substitutions, alter ligand receptor binding affinity. Prior experiments revealed IL-20R2 binds tighter to IL-19 and IL-20 than IL-20R1 (7, 31). However, in contrast to ∼1 nM IL-10/IL-10R1 and IL-22/IL-22R1 affinities (Table S7), IL-19/IL-20R2 and IL-20/IL-20R2 interactions are at least ∼100-fold weaker. Thus, in contrast to IL-10/IL-10R1 and IL-22/IL-22R1 complexes (Fig. 1), the IL-20R2 chain does not dominate ligand binding energetics, but must rely on cooperation between IL-20R1 and IL-20R2 to assemble the signaling complex. This property may allow the type-I receptor heterodimer (Fig. 1) to selectively discriminate IL-19, IL-20, and IL-24 affinity differences and induce distinct cellular responses. Using SPR (Fig. 6), the stability of the IL-20 type-I and type-II complexes were found to be more stable than the IL-19 type-I complex (Figs. 1 and 6). The molecular stabilities of the ternary complexes (IL-20 > IL-19) are consistent with robust IL-20 signaling in keratinocytes and its putative role in psoriasis, properties not shared by IL-19 (1, 7).

The presence of an IL-20/IL-20R1/IL-20R2 dimer in the crystals (Fig. 2*D*) provided a possible explanation for how IL-20SFCs might signal on immune cells in the absence of IL-20R1 (20, 22, 27). However, we could not generate biochemical evidence to confirm IL-19 or IL-20 can dimerize IL-20R2 in the absence of IL-20R1 (*SI Materials and Methods* and Fig. S4). Our studies suggest the main signaling unit of IL-19 and IL-20 are the ternary complexes, which may further oligomerize on cells. How the IL-20SFCs induce signals on immune cells, apparently in the absence of IL-20R1, remains to be elucidated (20, 27).

Materials and Methods

Protein Expression and Purification of the Complex. IL-20 (residues 25–176, uniprot Q9NYY1) was expressed with an N-terminal histidine tag in insect cells. IL-20R1 (residues 29–245, uniprot Q9UHF4), and IL-20R2 (residues 30–231, uniprot Q6UXL0) were expressed in insect cells with C-terminal histidine tags. Two *N*-linked glycosylation attachment sites in IL-20R2, (Asn-40$^{IL\text{-}20R2}$ and Asn-134$^{IL\text{-}20R2}$) were removed by mutagenesis (Quick Change; Stratagene) converting the asparagines to glutamines to yield IL-20R2^{QQ}, used for crystallization studies. IL-20R1 was modified by mutation of Lys-111$^{IL\text{-}20R1}$ and Lys-113$^{IL\text{-}20R1}$ to arginines (IL-20R1^{RR}) for crystallization. IL-20, and the receptors, were purified by nickel affinity chromatography. The histidine tags of all three proteins were removed by incubation with FactorXa protease. The

individual proteins were incubated at approximately a 1:1:1 stoichiometric ratio and purified by gel filtration chromatography. Fractions containing the ternary complex were concentrated to 7 mg/mL for crystallization.

Crystallization, X-ray data collection and refinement, surface plasmon resonance, and SAXS experiments are described in *SI Materials and Methods*.

ACKNOWLEDGMENTS. We thank Jean-Christophe Renauld for IL-20R2 cDNA, Sergei Kotenko for IL-20R1 cDNA, and Joshua LaBaer, Institute of Proteomics, Harvard Medical School, for IL-20 cDNA. This work was funded by National Institutes of Health Grants RO1-AI047300 and AI0473-S1 (to M.R.W.) The Advanced Photon Source, Southeastern Collaborative Access Team, beamline ID-22 is supported by contract no. W-31-109-Eng-38. Structure factors and coordinates have been deposited in the Protein Data Bank (accession nos. rcsb070584 and 4DOH). Usage of the Biacore T-200 is made possible by the University of Alabama at Birmingham Multidisciplinary Molecular Interaction Core. The Structurally Integrated BiologY for Life Sciences beamline is supported by the Department of Energy via the Integrated Diffraction Analysis Grant (DE-AC02-05CH11231).

1. Blumberg H, et al. (2001) Interleukin 20: Discovery, receptor identification, and role in epidermal function. *Cell* 104:9–19.
2. Chang C, et al. (2003) Crystal structure of interleukin-19 defines a new subfamily of helical cytokines. *J Biol Chem* 278:3308–3313.
3. Kunz S, et al. (2006) Interleukin (IL)-19, IL-20 and IL-24 are produced by and act on keratinocytes and are distinct from classical ILs. *Exp Dermatol* 15:991–1004.
4. Walter MR (2004) Structural analysis of IL-10 and Type I interferon family members and their complexes with receptor. *Adv Protein Chem* 68:171–223.
5. Pestka S, et al. (2004) Interleukin-10 and related cytokines and receptors. *Annu Rev Immunol* 22:929–979.
6. Dumoutier L, Leemans C, Lejeune D, Kotenko SV, Renauld JC (2001) Cutting edge: STAT activation by IL-19, IL-20 and mda-7 through IL-20 receptor complexes of two types. *J Immunol* 167:3545–3549.
7. Parrish-Novak J, et al. (2002) Interleukins 19, 20, and 24 signal through two distinct receptor complexes. Differences in receptor-ligand interactions mediate unique biological functions. *J Biol Chem* 277:47517–47523.
8. Sheikh F, et al. (2004) Cutting edge: IL-26 signals through a novel receptor complex composed of IL-20 receptor 1 and IL-10 receptor 2. *J Immunol* 172:2006–2010.
9. Kotenko SV, et al. (2001) Identification of the functional interleukin-22 (IL-22) receptor complex: The IL-10R2 chain (IL-10Rbeta) is a common chain of both the IL-10 and IL-22 (IL-10-related T cell-derived inducible factor, IL-TIF) receptor complexes. *J Biol Chem* 276:2725–2732.
10. Xie MH, et al. (2000) Interleukin (IL)-22, a novel human cytokine that signals through the interferon receptor-related proteins CRF2-4 and IL-22R. *J Biol Chem* 275: 31335–31339.
11. Chan JR, et al. (2006) IL-23 stimulates epidermal hyperplasia via TNF and IL-20R2-dependent mechanisms with implications for psoriasis pathogenesis. *J Exp Med* 203: 2577–2587.
12. Stenderup K, et al. (2009) Interleukin-20 plays a critical role in maintenance and development of psoriasis in the human xenograft transplantation model. *Br J Dermatol* 160:284–296.
13. He M, Liang P (2010) IL-24 transgenic mice: In vivo evidence of overlapping functions for IL-20, IL-22, and IL-24 in the epidermis. *J Immunol* 184:1793–1798.
14. Hsu YH, et al. (2006) Function of interleukin-20 as a proinflammatory molecule in rheumatoid and experimental arthritis. *Arthritis Rheum* 54:2722–2733.
15. Chen WY, Cheng BC, Jiang MJ, Hsieh MY, Chang MS (2006) IL-20 is expressed in atherosclerosis plaques and promotes atherosclerosis in apolipoprotein E-deficient mice. *Arterioscler Thromb Vasc Biol* 26:2090–2095.
16. Tritsaris K, et al. (2007) IL-20 is an arteriogenic cytokine that remodels collateral networks and improves functions of ischemic hind limbs. *Proc Natl Acad Sci USA* 104: 15364–15369.
17. Hsu YH, et al. (2011) Anti-IL-20 monoclonal antibody inhibits the differentiation of osteoclasts and protects against osteoporotic bone loss. *J Exp Med* 208:1849–1861.
18. Wolk K, Kunz S, Asadullah K, Sabat R (2002) Cutting edge: Immune cells as sources and targets of the IL-10 family members? *J Immunol* 168:5397–5402.
19. Wolk K, et al. (2008) Maturing dendritic cells are an important source of IL-29 and IL-20 that may cooperatively increase the innate immunity of keratinocytes. *J Leukoc Biol* 83:1181–1193.
20. Gallagher G (2010) Interleukin-19: Multiple roles in immune regulation and disease. *Cytokine Growth Factor Rev* 21:345–352.
21. Oral HB, et al. (2006) Regulation of T cells and cytokines by the interleukin-10 (IL-10)-family cytokines IL-19, IL-20, IL-22, IL-24 and IL-26. *Eur J Immunol* 36:380–388.
22. Wahl C, et al. (2009) IL-20 receptor 2 signaling down-regulates antigen-specific T cell responses. *J Immunol* 182:802–810.
23. Josephson K, Logsdon NJ, Walter MR (2001) Crystal structure of the IL-10/IL-10R1 complex reveals a shared receptor binding site. *Immunity* 15:35–46.
24. Jones BC, Logsdon NJ, Walter MR (2008) Structure of IL-22 bound to its high-affinity IL-22R1 chain. *Structure* 16:1333–1344.
25. Yoon SI, et al. (2010) Structure and mechanism of receptor sharing by the IL-10R2 common chain. *Structure* 18:638–648.
26. Bleicher L, et al. (2008) Crystal structure of the IL-22/IL-22R1 complex and its implications for the IL-22 signaling mechanism. *FEBS Lett* 582:2985–2992.
27. Nagalakshmi ML, Murphy E, McClanahan T, de Waal Malefyt R (2004) Expression patterns of IL-10 ligand and receptor gene families provide leads for biological characterization. *Int Immunopharmacol* 4:577–592.
28. Yoon SI, Logsdon NJ, Sheikh F, Donnelly RP, Walter MR (2006) Conformational changes mediate interleukin-10 receptor 2 (IL-10R2) binding to IL-10 and assembly of the signaling complex. *J Biol Chem* 281:35088–35096.
29. de Vos AM, Ultsch M, Kossiakoff AA (1992) Human growth hormone and extracellular domain of its receptor: Crystal structure of the complex. *Science* 255:306–312.
30. Boulanger MJ, Chow DC, Brevnova EE, Garcia KC (2003) Hexameric structure and assembly of the interleukin-6/IL-6 alpha-receptor/gp130 complex. *Science* 300: 2101–2104.
31. Pletnev S, et al. (2003) Characterization of the recombinant extracellular domains of human interleukin-20 receptors and their complexes with interleukin-19 and interleukin-20. *Biochemistry* 42:12617–12624.